ANU-P/676
June 1977

Recoil-distance lifetime measurements of the ground-state band in ^{164}Dy, ^{170}Er and ^{174}Yb

S.H. Sie and D.W. Gebbie

Department of Nuclear Physics,
Australian National University, Canberra, A.C.T., 2600, Australia.

Accepted for publication in Nuclear Physics.

Recoil-distance lifetime measurements of the ground-state band in ^{164}Dy, ^{170}Er and ^{174}Yb.

S.H. Sie and D.W. Gebbie

Department of Nuclear Physics, Research School of Physical Sciences, Australian National University, Canberra, ACT, 2600, Australia.

Abstract: Mean-lives of the 4^+, 6^+ and 8^+ levels of the ground-state band in ^{164}Dy, ^{170}Er and ^{174}Yb have been measured by the recoil-distance technique following multiple Coulomb excitation with ^{32}S projectiles of energy 120-140 MeV. The gamma-rays were detected in coincidence with backscattered particles. The results are compared with theoretical predictions of the adiabatic rotor model. The 6^+ and 8^+ lifetimes in ^{164}Dy are found to correspond to a slight reduction in B(E2) values over the rotational model prediction, while for the 4^+ state a 12% reduction was observed. In ^{170}Er and ^{174}Yb the lifetimes are consistent with rotational model predictions with a slight enhancement of B(E2) values at higher spins. Comparison with other results from Doppler broadened lineshape analysis confirms the need to adjust the electronic stopping powers of Northcliffe and Schilling in the lineshape calculations.

NUCLEAR REACTIONS ^{164}Dy, ^{170}Er, ^{174}Yb(^{32}S, ^{32}S'γ); E E = 120, 121, 140 MeV; measured recoil distance. ^{164}Dy, ^{170}Er, ^{174}Yb deduced $T_{1/2}$. Separated isotopes.

1. INTRODUCTION

As the number of high-spin (I > 6) states in heavy nuclei (A > 100) become more abundant and phenomena generally known as backbending become more familiar[1], more quantitative studies, in particular measurements of the transition matrix elements, become more desirable. These measurements, especially in the vicinity of the levels where backbending occurs, are crucial not only in understanding the mechanism involved, but may also help identify the members of the "superconducting" and yrast levels in the region of critical spin. At present, the small amount of lifetime data available generally have too poor an accuracy to make meaningful comparison with the various theories.

It has been known for some time that levels in the ground-state bands of the rare earths a few units of angular momentum below the critical spin deviate from the adiabatic rotor description by varying degrees. The deviations are especially strong in the lower transition region [2-4] and are attributable to various effects such as centrifugal stretching and band mixing. Although the deviations are less pronounced in the main region, it is of interest to determine their systematics, e.g., whether they correspond to positive (enhancement of the B(E2) over the rotational values) or to negative (reduction of the same) stretching.

The lifetimes or B(E2) values of these states lie in the region amenable to measurement by mainly three techniques; the recoil distance[5] (RD) method for mean-lives $10^{-12} \lesssim \tau \lesssim 10^{-9}$ s, the Doppler broadened lineshape analysis[6] (DBLS) and yield measurements from multiple Coulomb excitation (CE).

The lifetimes of the higher spin states (I > 10) are generally too short for the RD technique and, when (HI,xn) reactions are used to populate them[7], the measurements are further complicated by the feeding time[8] which often is comparable or longer than the lifetime of the level

itself. With the feasibility of Coulomb exciting the levels in the "backbending" region with very heavy ions[9] where large recoil velocities are involved, the DBLS method becomes more promising as a means to measure the lifetimes. Yield measurements following CE are in principle applicable, but the analysis becomes complicated with the increasing number of matrix elements (E2 and higher order) between the levels involved in the excitation and also by the inadequacy of the semi-classical calculation[10] presently used in the analysis due to the need for increasing quantal corrections[11].

The DBLS measurements have been successfully applied[6,12-15] following Coulomb excitation in several cases from which it became apparent that knowledge of the stopping power is the crux of the analysis. It was shown that for Sm and Gd recoiling in the range of velocities up to $\sim$ 4% C, the data suggests that the semi-empirical electronic stopping power values of Northcliffe and Schilling (NS)[16] are too low by as much as 30%[12]. This is consistent with empirical values given by Ziegler and Chu[17] from measurements of α-particle stopping powers in various media.

Several DBLS measurements have relied on NS for the electronic stopping powers or more recently on hybrid values[14,15] in which the NS values were normalised to include the medium dependences given by Ziegler and Chu[17]. The two sets of results show systematic discrepancies which point to the need for a set of lifetimes against which the dE/dx used in the lineshape calculation could be calibrated.

The recoil distance method provides the most direct means of lifetime measurement, with the additional advantage that it is applicable in a considerable range of lifetimes where the DBLS technique is also applicable.

This paper reports on recoil distance measurements of the 4^+, 6^+ and 8^+ members of the ground-state bands in ^{164}Dy, ^{170}Er and ^{174}Yb following

Coulomb excitation with ^{32}S ions. Deviations of the results from the adiabatic rotor model predictions are discussed and a comparison with other measurements is presented.

2. EXPERIMENTAL METHOD

The recoil-distance apparatus used in the present measurement is similar to that described in detail in refs.[3,18] and is shown schematically in fig. 1. The target consists of enriched isotope evaporated to a thickness of 1-2 mg/cm^2 onto a tightly stretched 500 μg/cm^2 Ni foil on the side facing the beam. The isotopic abundances of the targets are shown in table 1. The recoiling nuclei are stopped in a movable stopper mounted on a goniometer. A fine micrometer (readable to better than 1.25 μm) is used to position the stopper. Two kinds of stoppers were used in the experiment; one consists of a 2.5 mm thick polished Al plate covered with ∿ 15 mg/cm^2 of electroplated Ni and the other of a 0.5 mm thick polished Au disc with a ∿ 20 mg/cm^2 Pb layer deposited by evaporation.

The target-stopper distance is monitored by the capacitance measuring pulser system for separations of less than 200 μm, beyond which the response becomes insensitive and non-linear. The limit of minimum distance, defined when the stopper makes contact with the target, is determined mainly by the limit of flatness of the target. In the present experiment separations of less than 30 μm were achieved and stability of distance was better than 2 μm.

The γ-rays were detected at 0° with respect to the beam direction in a 50 cm^3 Ge(Li) counter in coincidence with particles backscattered into an annular counter subtending an angular range of 155 - 170°. The resolution of the Ge(Li) counter was 2.0 keV for the 344 keV γ-ray in ^{152}Eu. The same source was used to calibrate the photopeak efficiency of the counter. A 500 μg/cm^2 Ni foil was used to cover the particle detector to reduce the counting rate due to radiation other than the backscattered ions of interest.

The data were collected in an on-line NP2100 computer with the γ-rays, particles, TAC and, in the case of small distances, the monitor pulser, stored event by event on magnetic tape.

A beam of ^{32}S with energies of 120 - 140 MeV from the ANU 14UD Pelletron was used to Coulomb excite the target. Beam currents up to 100 na of either 10^+ or 11^+ charge state were used. Two sets of measurements each were carried out at 121, 120 and 125 MeV for ^{164}Dy, ^{170}Er and ^{174}Yb respectively and one each at 140 MeV for the ^{170}Er and ^{174}Yb targets. Partial level diagrams for these nuclei are shown in fig. 2 and typical spectra obtained are shown in figs. 3 - 5. Recoil velocities, corresponding to $\beta = \frac{v}{c}$ of between 2.0 - 2.4% were obtained which agree reasonably well with those calculated kinematically with some allowance for energy loss due to the target thickness and to the stretched Ni foil backing. At these recoil velocities the Ge(Li) detector completely resolved the Doppler shifted γ-rays (emitted in vacuum) from the unshifted γ-rays (emitted after the recoils are stopped) for the $8^+ \rightarrow 6^+$ transitions. For the $6^+ \rightarrow 4^+$ and $4^+ \rightarrow 2^+$ transitions, the resolution was not complete but was more than adequate to facilitate extraction of the experimental quantity $f = u/(u + s)$, where u and s are respectively the unshifted and the shifted photopeak areas of the γ-ray. The background under the peak was determined by the method described e.g., in refs.[12,15] and is such that the number of background counts in any channel is proportional to the area of the peak accumulated from the high-energy side. Random coincidences were subtracted prior to extraction of peak areas.

For the $8^+ \rightarrow 6^+$ transitions with short lifetimes ($\tau < 10$ ps) a considerable amount of Doppler broadening of the "unshifted" peak occurs due to the finite stopping time (~ 1 ps) of the recoils in the stopper,

thus leaving a portion of the unshifted peak under the fully shifted peak. Two methods were used to determine this amount. In the first one, the amount is determined from the calculated Doppler broadened lineshape using lifetimes derived from initial analysis. In the second method, a Gaussian is generated from points on the high-energy side of the shifted peak. The two methods agree well and introduce only minor corrections to the quantity f. Corrections due both to relativistic effects on solid angle and to photopeak detection efficiency (due to distance and energy) were applied to f prior to least squares fitting of the decay curve. In the simplest case of transitions originating from a level not fed by cascade, $f = e^{-t/\tau}$ where τ is the mean lifetime of the state and t is the time of recoil in vacuum. A plot of log f versus t (or target stopper distance $d = \beta ct$) would be a straight line. Deviations from a straight line near f = 1 are due, as can be seen in figs. 6 - 9, to cascade feeding from other levels. Deorientation effects[19] were included in the decay curve. In the present experiment, the cascade feeding constituted a major portion of the $4^+ \rightarrow 2^+$ transition and to a lesser extent that of the $6^+ \rightarrow 4^+$ transition as well. Assuming that the deorientation follows[19,20] $A_k = e^{-\eta_k t} A_{k0}$, where A_{k0} are the usual angular distribution coefficients ($W(\theta) = 1 + \sum_k Q_k A_{k0} P_k(\cos\theta)$), the effect of deorientation of both the feeding (2) and fed level (1) to the decay of the latter is given by

$$f = \frac{e^{-\lambda_1 t} + R_2 \dfrac{\lambda_2 e^{-\lambda_1 t} - \lambda_1 e^{-\lambda_2 t}}{\lambda_1 - \lambda_2} + \sum_k \bar{G}_k W_k \left[\rho_k(1) e^{-\lambda_{1k} t} + R_2 \rho_k'(2) \dfrac{\lambda_2 e^{-\lambda_{1k} t} - \lambda_1 e^{-\lambda_{2k} t}}{\lambda_{2k} - \lambda_{1k}} \right]}{1 + R_2 + \sum_k W_k \left(\rho_k(1)\, g_k(1) + R_2\, \rho_k'(2) \dfrac{\lambda_2 g_k(1) - \lambda_1 g_k(2)}{\lambda_{2k} - \lambda_{1k}} \right)}$$

where

$$\lambda_{ik} \equiv \lambda_i + \eta_k(i) \quad , \qquad W_k = F_k\, Q_k\, P_k(\cos\theta),$$

$$g_k(i) \equiv \bar{G}_k e^{-\lambda_{ik} t} + \frac{\lambda_i}{\lambda_{ik}} \left(1 - e^{-\lambda_{ik} t}\right), \quad \rho_k'(2) = U_k(2 \rightarrow 1)\, \rho_k(2) \quad ,$$

the λ's are the decay constants ($= \frac{1}{\tau}$) of the levels, the η's are the deorientation constants, ρ_k are the statistical tensors describing the initial alignment of the level[21], F_k are the F coefficients of the γ-decay of level 1, Q_k are the solid angle attenuation coefficients, P_k are the Legendre polynomials of order k, U_k are the dealignment factors[21] of level 2, R_2 is the ratio of the initial population of level (2) to that of level (1) and $\overline{G}_k$ are the integral attenuation coefficients for the stopped decay. Since the effect of deorientation is not too large, deorientation due to triple cascade can be neglected, especially considering the fact that in the present case the lifetimes of successive feeding levels decrease very rapidly with increasing level energy. Differential measurements[19] and a recent integral measurement[22] of the deorientation effect showed that the ratio of η_2/η_4 is consistent with a magnetic dipole interaction with a mixture of quadrupole interaction. In the present analysis η values from ref.[22] were adopted. For the nickel stopper, values for $\overline{G}_k$ were obtained from ref.[3] and no attenuation was assumed for the lead stopper. Variations of as much as 50% in these constants resulted in less than a 1% change in the derived lifetimes. Values for the feeding ratio R were derived experimentally and in table 2 they are compared with those calculated from the Winther-de Boer program using the rotational matrix elements. The statistical tensors ρ_k for Coulomb excitation in the backscattering mode are given by $\rho_k = \sqrt{2k+1}\,\alpha_{k0}/\alpha_{00}$, where the α_{k0}'s were calculated with the Winther-de Boer program[10].

The fitting proceeded first with the 8^+ state, for which calculated values of the lifetime of the 10^+ state were used. An iterative procedure was used in deriving the final values. The zero distance, lifetimes, populations of the levels as well as the deorientation constants can be varied in the least squares fitting. In the final analysis only the zero distance and the lifetime of the level of interest were fitted. The zero

distance obtained from the fit for various levels within one set of measurements agreed with that derived from the pulser system measurements.

The conversion of distance scale to time scale was made using the measured recoil velocities as derived from the observed Doppler shifts according to formulae given, e.g., in ref.[4]. Within the same nucleus, kinematically the average recoil velocities should decrease with increasing energy of the level excited, but the spread in recoil energy for all levels ($\leq$ 0.1%) results in much smaller error than that of the observed energy shifts. In each measurement a weighted average of the recoil velocities for the 8^+, 6^+ and 4^+ states was used in the conversion shown in table 2. The measured recoil velocities agree well (better than 5%) with values derived from kinematics and estimates of the energy loss in the target and backing.

In the absence of isomeric feeding a plot of log f vs. distance should follow an almost straight line with slight adjustment due to cascade feeding, but as can be seen in figs. 7, 8, the curves for the $6^+ \rightarrow 4^+$ transitions in ^{170}Er and ^{174}Yb and for the $8^+ \rightarrow 6^+$ in ^{174}Yb appear to reach a constant "background" level at distances corresponding to $t \gtrsim 5\tau$. This could be attributed to the difficulty in extracting the unshifted peak areas once they become comparable to the statistical uncertainty (usually of the order of 2%) and also to the presence of peaks due to impurities in the target. In the present experiment the ^{164}Dy, ^{170}Er and ^{174}Yb targets were enriched to 98.4%, 96.9% and 95.8% respectively; the enrichments are shown in table 1 together with those for the main impurities. To better determine the level of this "background" for the various transitions, several runs corresponding to flight times of $t \gtrsim 5\tau$ were summed prior to extraction of the peak areas. This background level, hereafter referred to as f_∞, varied between 1 - 2%, the highest being that for the $6 \rightarrow 4$ transition in ^{174}Yb. An error in f_∞ of 0.01 translates to a relative error in τ of $\Delta\tau/\tau \approx c\Delta f \approx 2.7\%$.

In all cases except for the $8^+ \rightarrow 6^+$ (373.7 keV) transition in ^{170}Er

and the $4^+ \rightarrow 2^+$ transitions in ^{164}Dy (168.8 keV) and in ^{174}Yb (176.6 keV), the known transitions from the impurities are well separated from the transition of interest and are not likely to cause errors in f at large distances. The Doppler-shifted photopeak of the $8^+ \rightarrow 6^+$ transition in ^{166}Er (τ = 6.9 ps, ref.[13]), assuming the same shift as that observed for the corresponding $8^+ \rightarrow 6^+$ transition in ^{170}Er, appeared $\sim$ 1 keV above the unshifted part of the latter. The contribution from this estimated from measurement at large distances agrees with that estimated from the given abundance of ^{166}Er in the target ($\sim$ 0.9%). Corrections to f measured at shorter distances were made using the known lifetime of the 8^+ state in ^{166}Er. In the ^{164}Dy case, a ground-state transition from a level in ^{163}Dy at 167.3 keV ($T_{1/2}$ = 420 ps, ref.[23]) interferes with the $4^+ \rightarrow 2^+$ transition. From the measured small intensity of a 93.9 keV transition depopulating the same level in ^{163}Dy and from the known branching ratio $I_\gamma(167.3)/I_\gamma(93.9)$, an upper limit of 0.3% was obtained for the intensity of the 167.3 keV γ-ray in the $4^+ \rightarrow 2^+$ transition in ^{164}Dy. A correction for this was applied with very minimal effect on the decay curve of the latter. In the ^{174}Yb case, the $\sim$ 1% amount of ^{173}Yb in the target gave a 179.3 keV γ-ray from Coulomb excitation originating from the 179.3 keV level (τ = 461 ps, ref.[23a]). The contribution of this peak was determined from measurement at large distances and, using its known lifetime, was subtracted from f for the $4^+ \rightarrow 2^+$ transition in ^{174}Yb.

A plausible explanation for the relatively high level of f_∞ for the ^{174}Yb $6^+ \rightarrow 4^+$ transition is that it is caused by feeding from the isomeric level at 1.518 MeV excitation. This state has been observed previously[24] and is interpreted as being a K-isomer ($KJ^\pi = 6^6^+$) with a half-life of 860 μs. This state decays mainly to the 8^+, 6^+ and 4^+ states of the ground-state band with 2.4, 84 and 2% branches respectively. Thus if f_∞ in ^{174}Yb is due to feeding from this isomeric state, it is expected that

$f_{\infty}(8^+) = \frac{2.4\%}{84\%} \times P(6^+)/P(8^+) \times f_{\infty}(6^+)$, where P(I) denotes the excitation probability of level I, giving $f_{\infty}(8^+) = 0.2\%$ and 0.14% for the data taken at 125 MeV and at 140 MeV bombarding energies respectively. These values are reasonably consistent with observation as can be seen in fig. 8. The isomeric feeding would appear in the $4^+ \rightarrow 2^+$ transition mainly from cascade from the 6^+ state and thus $f_{\infty}(4^+) = f_{\infty}(6^+) \times R(4^+)/(1+R(4^+)) = 1\%$ and 2.2% at 125 and 140 MeV respectively. Here $R(4^+)$ is the feeding ratio for the 4^+ state as tabulated in table 2. In fitting the $4^+ \rightarrow 2^+$ decay curves, $f_{\infty}(4^+)$ together with a 50% uncertainty was included. The isomeric state could presumably be fed by cascade from higher-lying, high-spin states. It is interesting to note that a similar K-isomer in ^{176}Yb at 1.041 MeV ($KJ^{\pi} = 8^+$, $T_{1/2}$ = 11 s) was observed in recent Coulomb excitation measurements with Xe and Kr ions[14]. A similar K-isomer was predicted[24] for ^{170}Er although as yet there is no report on its observation.

3. RESULTS

The results for the mean-lives of the 4^+, 6^+ and 8^+ states are shown in table 3. The errors shown are standard deviations from the fit and include errors due to the uncertainties in the deorientation time constants and feeding corrections.

Results from two separate measurements in ^{164}Dy at 121 MeV are in good agreement and in ^{170}Er the two measurements at 120 MeV agree with that done at 140 MeV beam energy. Similarly, in ^{174}Yb the results of two measurements at 125 MeV agree with that measured at 140 MeV. The results obtained from the several sets are averaged and shown in column 7 of the table.

Lifetimes from previous measurements were obtained mainly from DBLS analysis. In ^{164}Dy two of the three available DBLS values for the 8^+ state agree with the present result. In ^{170}Er the

only DBLS measurement available for the 8^+ state is in good agreement with the present result. In ^{174}Yb two DBLS values are available for the 8^+ and one for the 6^+ state. In the measurements by Ward et al.[14] the Northcliffe and Schilling[16] electronic dE/dx values were modified to allow for the media dependence given by Ziegler and Chu[17]. The Yb in Yb values given by NS, at a given MeV/amu, were scaled by the discrepancy between the NS and ZC tables for α-particles at the same value of MeV/amu. This correction amounted to only about 5%, in contrast to the large one (∿ 30%) for the case of Sm and Gd[12]. The result for the 8^+ state in ^{174}Yb following such a procedure agrees very well with the present result, while the other result from Kearns et al.[13] for which no such correction was applied is larger. The latter data were taken in singles only and, as pointed out by Ward[1], singles lifetimes appear to differ systematically from those obtained from coincidence measurements. It should be noted here that the normalization of dE/dx works in Th as well[15].

No lifetime measurements are available to compare with the remaining 6^+ and 4^+ states studied here. Some information on these states is obtained from Coulomb excitation yield measurements[34,36]. For comparison with the present results the available B(E2) values were converted into mean-lifetimes. The electron conversion coefficients were taken from the Hager and Seltzer tables[25] and are shown in column 4 of table 2. Finally the last column shows the rigid-rotor predictions corresponding to B(E2) values projected from the $B(E2;0\rightarrow 2)$ shown in table 2 according to

$$B(E2;1\rightarrow J)_{rot} = 5B(E2;2\rightarrow 0)\langle I020;J0\rangle^2$$

where $J = I-2$.

The present result for the 4^+ state mean-life in ^{164}Dy is significantly longer (∿ 12%) than that from CE measurements[34] which in turn agree with the rotational model prediction. The present results for the 6^+ and 8^+

states however are consistent with the CE results and are slightly longer than the rotational model prediction. The CE results in ^{164}Dy included corrections for excitation of vibrational states, quantal effects and E4 moments which for the 4^+ state amounted to $\sim$ -3.2%, -1% and -2.9% respectively. Allowing for reasonable uncertainties in these corrections, the discrepancy with the present result is rather large. A recent recoil-distance measurement[35] in ^{162}Dy shows good agreement with the CE result for the 4^+ state. In order to check on the possibility of systematic error in the present measurements, a run with a natural Dy target was carried out with 121 MeV ^{32}S. The target was prepared from 99.9% pure Dy metal rolled into a 2.2 mg/cm^2 foil which was then stretched in the usual manner. The results for the 6^+ state in ^{164}Dy agree closely with the measurements on the separated ^{164}Dy targets and the 4^+ lifetime in ^{162}Dy agrees with that reported by Johnson et al.[35] to within 3%. Unfortunately the $4^+ \rightarrow 2^+$ transition from ^{164}Dy was heavily contaminated by the ground-state transition from the 167.3 keV level in ^{163}Dy which, since the lifetime is poorly known, prevented accurate extraction of τ_{4^+}. However within large uncertainty the result is consistent with that shown in table 3. A detailed report of this experiment will be given elsewhere.

It is possible that the B(E2;$0 \rightarrow 2$) in ^{164}Dy used in calculating the rotational values is too high, although it appears to be reasonable from the systematics of the even Dy isotopes. A possible error of 3% in the total conversion coefficient as pointed out, e.g., by Guidry et al.[15], actually would result in better agreement between the different B(E2;$0 \rightarrow 2$) values from timing and inelastic scattering experiments.

In ^{170}Er the present result for the 4^+ state is consistent with the rotational model. The 6^+ and 8^+ state lifetimes are slightly shorter than the rotational model values indicating enhancement of the B(E2) values. No other B(E2) data are available.

The situation in ^{174}Yb is similar to that in ^{170}Er; the 4^+ lifetime is consistent with the rotational prediction while the 6^+ and 8^+ values correspond to slight enhancement of the B(E2) values. Some data from CE[36] are available for the 4^+ and 6^+ states but since no quantal and E4 corrections were applied in the analysis these are thus excluded from the present compilation.

In table 4 the B(E2) values derived from the present lifetime values are presented together with the rotational B(E2) values projected from the adopted B(E2;0→2) values. The last column gives the ratio $B(E2)/B(E2)_{rot}$ from both the present experiment including the error in the B(E2;0→2), and other values from DBLS measurements.

All the nuclei presently studied are usually described as "good" rotors, so defined when the coefficients in the expansion of the energy levels of the ground-state band

$$E(I) = E_0 + AI(I+1) + B[I(I+1)]^2 \qquad (1)$$

are such that $|B/A| \approx 10^{-3}$. The observed deviations correspond to negative values of B and can be attributed to various effects such as Coriolis anti-pairing, fourth-order cranking, centrifugal stretching and band-mixing. Corresponding deviations of the B(E2) values in the ground-state band can be written as

$$B(E2;I \to I-2) = B(E2;I \to I-2)_{rot}\,[1 + \alpha(I^2 - I - 2)]^2 \ . \qquad (2)$$

Such a single-parameter fit works rather well for most of the even-even rare-earths. For the "good" rotors ^{154}Sm and ^{156}Gd, $\alpha \approx 1 \times 10^{-3}$ and can be attributed mainly to mixing with the β-band. Fig. 10 shows a plot of $B(E2)_{exp}/B(E2)_{rot}$ from the present experiment and from other results from DBLS measurements. The latter provided B(E2) values up to spin 14 in ^{164}Dy and ^{174}Yb and to spin 12 in ^{170}Er. The curves shown represent

eq. (2) with $\alpha = \pm 1 \times 10^{-3}$. While there appears to be considerable scatter in the data points, the higher spin data indicate that the B(E2) values are well within reasonable definition of being those of good rotors.

If the deviation from the rigid rotor is due to centrifugal stretching, parameter α can be related to the parameters in eq. (1) by $\alpha = -B/A$. From the energy spacing observed up to spin 12, $\alpha = +0.5 \times 10^{-3}$, 0.38×10^{-3} and 0.24×10^{-3} for ^{164}Dy, ^{170}Er and ^{174}Yb respectively, implying very little centrifugal stretching. The higher spin data ($I > 10$) from the DBLS measurements which are most sensitive to this effect appear to be consistent with these values. In ^{170}Er and in ^{174}Yb the deviations for the lower spin states as derived from the B(E2) values appear to be larger than at higher spin, which may indicate that while at lower spin these nuclei are somewhat "soft", they become more rigid at higher spin as maximum stretching is achieved. While this picture is plausible it does not account for the apparent reduction in B(E2) in ^{164}Dy especially below spin 8. Similar negative stretching was observed in ^{160}Dy and ^{162}Dy for the 6^+ and 8^+ states from CE measurements[35] as well as from DBLS measurements for spin $I > 8$. Uncertainties in both measurements are large, in the latter particularly due to the problem with the stopping powers. More accurate data are needed to confirm these results. Microscopic calculations based on the pairing-plus-quadrupole model by Kumar[37] for ^{160}Dy showed that the B(E2) values in the ground-state band increase gradually with spin up to spin 16 contrary to the available data.

While the fitted lifetimes are relatively insensitive to variation in the feeding ratios $R(I) \equiv \sum_{I_i > I} P(I_i)/P(I)$, where P(I) is the excitation probability of level I, the comparison of calculated and experimental R(I)'s should give additional independent information on the matrix elements. In table 2 two sets of R values are given for each case; one derived from the Winther-de Boer program calculation with adiabatic rotor matrix elements and the other

with the "stretched" matrix elements using the parameter $\alpha = 1.0 \times 10^{-5}$. For the lower bombarding energies the agreement of experimental $R(6^+)$ and $R(4^+)$ with the rotational values is excellent, while $R(8^+)$ suggests enhancement of the B(E2) values for $I \geq 8$. At 140 MeV both ^{170}Er and ^{174}Yb showed lower $R(6^+)$, indicating enhanced yield for the 6^+ state probably due to nuclear interference.

4. CONCLUSION

The results of recoil-distance measurements of lifetimes for the 4^+, 6^+ and 8^+ states in ^{164}Dy, ^{170}Er and ^{174}Yb have been presented. The results are consistent with a slight enhancement of the B(E2)'s over the rigid-rotor predictions, except in ^{164}Dy where a slight reduction was observed. Comparison of the results of recoil-distance with DBLS measurements confirm the need to renormalize the electronic dE/dx of NS, and corroborate the validity of a procedure first applied in the Sm case. Relative yield measurements well below the Coulomb barrier show results consistent with the lifetime measurements.

After the preparation of this paper, an extended report[38] on the measurements in ref.[13] appeared which includes revised values for the lifetimes and B(E2) values given in tables 3, 4.

We would like to thank Dr. R.M. Diamond for his helpful comments and suggestions. We would also like to thank Mr. A.F. Muggleton for producing the targets and Messrs. M.P. Fewell, A.B. Jones, J. Rayner and J. Soderbaum for help in collecting data at various stages of this work.

REFERENCES

1) D. Ward, Proc. Int. Conf. on Reactions between Complex Nuclei, Nashville, Vol.2 (North-Holland, Amsterdam 1975) p.417.

2) I.A. Fraser, J.S. Greenberg, S.H. Sie, R.G. Stokstad and D.A. Bromley, Phys.Rev.Lett. 23 (1969) 1047; 23 (1969) 1051.

3) N. Rud, G.T. Ewan, A. Christy, D. Ward, R.L. Graham and J.S. Geiger, Nucl.Phys. A195 (1972) 545.

4) R.M. Diamond, F.S. Stephens, K. Nakai and R. Nordhagen, Phys.Rev. C3 (1971) 344.

5) T.K. Alexander, K.W. Allen and D.C. Healy, Phys.Lett 20 (1965) 402.

6) R.G. Stokstad, I.A. Fraser, J.S. Greenberg, S.H. Sie and D.A. Bromley, Nucl.Phys. A156 (1970) 145.

7) D. Ward, H.R. Andrews, J.S. Geiger, R.L. Graham andJ.F. Sharpey-Schafer, Phys.Rev.Lett. 30 (1973) 493.

8) J.O. Newton, F.S. Stephens and R.M. Diamond, Nucl.Phys. A210 (1975) 19.

9) I-Y. Lee, R.S. Simon, P.A. Butler, P. Colombani, M.W. Guidry, F.S. Stephens, R.M. Diamond, N.R. Johnson and E. Eichler, Phys.Rev. Lett. 37 (1976) 420.

10) A. Winther and J. de Boer, in Coulomb Excitation (Academic Press, New York, 1966) p.303.

11) F. Rösel, J.X. Saladin and K. Alder, Comp.Phys.Comm. 8 (1974) 35.

12) S.H. Sie, H.R. Andrews, J.S. Geiger, R.L. Graham and D. Ward, Bull. Am.Phys.Soc. 17 (1972) 536; 18 (1973) 629; 18 (1973) 1597.

13) F. Kearns, G. Dracoulis, T. Inamura, J.C. Lisle and J.C. Willmott, J. of Phys. A7 (1974) L11.

14) D. Ward, P. Colombani, I-Y Lee, P.A. Butler, R.S. Simon, R.M. Diamond and F.S. Stephens, Nucl.Phys. A266 (1976) 194.

15) M.W. Guidry, P.A. Butler, P. Colombani, I-Y. Lee, D. Ward, R.M. Diamond and F.S. Stephens, Nucl.Phys. A266 (1976) 228.

16) L.C. Northcliffe and R.F. Schilling, Nuc. Data Tables A7 (1970) 23.

17) J.F. Ziegler and W.K. Chu, Atomic and Nucl. Data 13 (1974) 463.

18) T.K. Alexander and A. Bell, Nucl.Instr. & Meth. 81 (1970) 22.

19) D. Ward, R.L. Graham, J.S. Geiger, H.R. Andrews and S.H. Sie, Nucl.Phys. A193 (1972) 479.

20) H. Spehl, S.G. Steadman, A. Weckherlin, H.A. Soubt, K. Hagemeyer, G.J. Kumbartzki and K.H. Speidel, Nucl.Phys. A215 (1973) 446.

21) T. Yamazaki, Nuclear Data A3 (1967) 1.

22) D. Ward, H.R. Andrews, R.L. Graham, J.S. Geiger and N. Rud, Nucl.Phys. A234 (1974) 94.

23) A. Buyrn, Nucl. Data 8 (1972) 295 and refs. therein.

23a) B. Harmatz and D.J. Horen, Nucl.Data 14 (1975) 297 and refs. therein.

24) J. Borggreen, N.J. Hansen, J.P. Pedersen, L. Westgaard, J. Zylicz and S. Bjornholm, Nucl.Phys. A96 (1967) 561;
M.M. Minor, Nucl.Data 10 (1973) 515.

25) R.S. Hager and E.C. Seltzer, Nucl.Data A4 (1968) 1.

26) B. Elbek, M.C. Olesen and O. Skilbreid, Nucl.Phys. 19 (1960) 523.

27) K.A. Erb, J.E. Holden, I-Y. Lee, J.X. Saladin, T.K. Saylor, Phys.Rev.Lett. 29 (1972) 1010.

28) A.H. Shaw and J.S. Greenberg, Phys.Rev. C10 (1974) 263.

29) J.D. Kurfess, R.P. Scharenberg, Phys. Rev. 161 (1967) 1185.

30) F.W. Richter, J. Schutt, D. Wiegandt, Z. Physik 213 (1968) 202.

31) R. Avida, Y. Dar, P. Gilad, M.B. Goldberg, K.H. Speidel and Y. Wolfson, Nucl.Phys. A127 (1969) 412.

32) Y. Dar, S. Kochar and I. Tserruya, Phys.Rev. C7 (1973) 472.

33) G.B. Hagemann, D.C. Hensley, N.R. Johnson, W.T. Milner and L.L. Riedinger, Bull. Am.Phys.Soc. II 18 (1973) 581;
A. Buyrn, Nucl. Data 11 (1974) 327.

34) R.O. Sayer, E. Eichler, N.R. Johnson, D.C. Hensley and L.L. Riedinger, Phys. Rev. C9 (1974) 1103.

35) N.R. Johnson, P.P. Hubert and E. Eichler, Bull.Am.Phys.Soc. 21 (1976) 658.

36) R.O. Sayer, P.H. Stelson, F.K. McGowan, W.T. Milner and R.L. Robinson, Phys.Rev. C1 (1970) 1525.

37) K. Kumar, Phys.Rev.Lett. 30 (1973) 1227.

38) F. Kearns, G. Varley, G.D. Dracoulis, T. Inamura, J.C. Lisle and J.C. Willmott, Nucl.Phys. A278 (1977) 109.

TABLE 1.

Isotopic abundance of the targets

Dy	A	156	158	160	161	162	163	164
	%	<.01	<.01	.02	.15	.35	1.05	98.43
Er	A	162	164	166	167	168	170	
	%	.02	.04	.87	.72	1.46	96.89	
Yb	A	168	170	171	172	173	174	176
	%	<.01	.05	.41	.99	2.2	95.8	.57

TABLE 2

Feeding ratios and recoil velocities.

Nucleus	$B(E2;0^+\rightarrow 2^+)$ e^2b^2	^{32}S Ecam Energy (MeV)	Level I^π	R_I [a] (exp.)	$R_I(1)$ [b] (calc.)	$R_I(2)$ [c] (calc.)	Measured v/c
^{164}Dy	5.57(.04) [d]	121	4^+	1.20(.06)	1.300	1.392	
			6^+	.412(.018)	.392	.442	.0240 ± .0008
			8^+	.195(.019)	.183	.223	
^{170}Er	5.81(.09) [e]	120	4^+	.78 (.03)	.900	.955	
			6^+	.308(.012)	.297	.329	.02033 ± .00025
			8^+	.200(.014)	.140	.157	
		140	4^+	4.5 (.7)	4.31	4.65	
			6^+	.64(.03)	.849	.970	.0222 ± .001
			8^+	.267(.017)	.336	.414	

(continued)

TABLE 2 (continued)

^{174}Yb	5.92(.05)[f]	125	4^+	1.07 (.06)	1.058	1.089	
			6^+	.331(.011)	.337	.382	.0229 ± .0003
			8^+	.212(.010)	.158	.145	
		140	4^+	3.9 (.5)	3.31	3.56	
			6^+	.44(.02)	.722	.822	.0230 ± .0002
			8^+	.26(.02)	.298	.367	

a) $R_I \equiv \sum_{I'>I} Y(I')/Y(I)$, where Y(I) is the total yield of level I.

b) $R_I \equiv \sum_{I'>I} P(I')/P(I)$, where P(I) is the excitation probability of level I calculated with the Winther-de Boer program using rotational matrix elements.

c) Calculated as in b) using "stretched" matrix elements corresponding to $\alpha = 1.0 \times 10^{-3}$. See text.

d) Average of refs. [26,27,28].

e) Average of refs. [29,30,31].

f) Average of ref. [28,32].

TABLE 3.

Lifetimes of the ground-state band levels.

Nucleus	$I_i \rightarrow I_f$	E_γ (keV)	α_T [a]	τ_{I_i} (ps) (b)	(c)	(d)	Average	Other meas.	τ_{rot} [e]
^{164}Dy	$4^+ \rightarrow 2^+$	168.8	0.45	303(14)	289(11)		294(9)	260(30) [i]	258
	$6^+ \rightarrow 4^+$	259.1	0.102	36.7(1.7)	40.3(2.7)		37.7(1.4)	44.4(2.4) [i]	36.2
	$8^+ \rightarrow 6^+$	342.3	.0445	9.7(.7)	11(2)		9.8(.7)	11.7(.7) [i] 10.6(.9) [f] 9.12(.46) [g]	9.1
^{170}Er	$4^+ \rightarrow 2^+$	181.2	0.37	200(8)	199(10)	172(13)	196(5)		184
	$6^+ \rightarrow 4^+$	280.2	.091	20.3(1.1)	27.9(1.5)	22(3)	22.9(.9)		24.1
	$8^+ \rightarrow 6^+$	373.7	.038	5.5(.6)	7.7(1.4)	5.7(.5)	5.8(.4)	5.7(.6) [f]	5.7
^{174}Yb	$4^+ \rightarrow 2^+$	176.6	.42	216(11)	195(17)	195(11)	208(6)		198
	$6^+ \rightarrow 4^+$	272.9	.103	22.9(.7)	27(1.8)	25.6(3.5)	23.5(0.6)	20(.5) [h]	26
	$8^+ \rightarrow 6^+$	363.5	.044	5.3(.3)	5.1(.7)	5.2(1.0)	5.3(.3)	5.2(.7) [h] 6.3(.6) [f]	6.3

a) Total E2 Conversion Coefficient $\alpha_T = \alpha_K + 1.33\ \Sigma\alpha_L$, ref. [25].

b,c) Results for 121, 120, 125 MeV beam energy for ^{164}Dy, ^{170}Er, and ^{174}Yb, respectively.

d) Results for 140 MeV beam energy for ^{170}Er and ^{174}Yb.

e) Calculated using $B(E2;0^+ \rightarrow 2^+)$ from table 2.

f) Ref. [13].

g) Ref. [31].

h) Ref. [14].

i) Ref. [34].

TABLE 4

Summary of B(E2) values of the ground state-bands

Nucleus	I J	$B(E2;I\to J)_{exp}$ (e^2b^2)	$B(E2;I\to J)_{rot}$ (e^2b^2)	$\frac{B(E2)_{exp}}{B(E2)_{rot}}$
^{164}Dy	0^+ 2^+		5.57(0.04)	≡ 1.0
	2^+ 4^+	2.51(0.08)	2.86	0.88(0.03)
	4^+ 6^+	2.42(0.09)	2.52	0.96(0.04)
	6^+ 8^+	2.22(0.16)	2.39	0.93(0.07)
				1.0 (.07)[a]
				0.85(0.09)[b]
	8^+ 10^+		2.33	1.20(.13)[a]
				0.90(0.08)[b]
	10^+ 12^+		2.28	1.33(.16)[a]
				0.93(0.09)[b]
	12^+ 14^+		2.25	0.91(0.09)[b]
^{170}Er	0^+ 2^+		5.81(0.09)	≡ 1.0
	2^+ 4^+	2.80(0.07)	2.98	0.94(0.03)
	4^+ 6^+	2.78(0.12)	2.64	1.05(0.05)
	6^+ 8^+	2.46(0.18)	2.50	0.98(0.07)
				0.97(0.10)[b]
	8^+ 10^+		2.42	0.95(0.10)[b]
	10^+ 12^+		2.38	0.91(0.10)[b]
^{174}Yb	0^+ 2^+		5.92(0.05)	≡ 1.0
	2^+ 4^+	2.90(0.08)	3.05	0.95(0.03)
	4^+ 6^+	2.99(0.08)	2.70	1.11(0.03)

(cont'd..)

TABLE 4 (cont'd.)

			1.30(0.33)[c]
6^+ 8^+	3.04(0.17)	2.56	1.19(0.07)
			1.06(0.10)[b]
			1.22(0.16)[c]
8^+ 10^+		2.48	0.92(0.09)[b]
			1.03(0.10)[c]
10^+ 12^+		2.43	0.98(0.11)[b]
			1.05(0.11)[c]
12^+ 14^+		2.86	0.87(0.22)[c]

a) ref. 33

b) ref. 13

c) ref. 14

FIGURE CAPTIONS

Fig. 1. Schematic diagram of the recoil-distance apparatus. The gamma rays are detected at 0° with respect to the beam direction in coincidence with particles backscattered into the annular counter. The stopper is mounted on a goniometer to facilitate parallel alignment of the target and the stopper. The goniometer in turn is mounted on a sliding stage positioned by a fine micrometer. Target-stopper distance is monitored by a pulser system sampling the capacitance.

Fig. 2. Partial level diagram of ^{164}Dy, ^{170}Er and ^{174}Yb showing members of the ground-state band populated in the present experiments.

Fig. 3. Gamma-ray spectra of ^{164}Dy observed in coincidence with backscattered ^{32}S projectiles for 121 MeV bombarding energy at different settings of the stopper-target distance d.

Fig. 4. Gamma-ray spectra of ^{170}Er for 120 MeV ^{32}S at different settings of d.

Fig. 5. Gamma-ray spectra of ^{174}Yb for 125 MeV ^{32}S at different settings of d.

Fig. 6. Decay curves of the 4^+, 6^+ and 8^+ states in ^{164}Dy for 121 MeV ^{32}S beam. The log of the quantity $f = u/u+s$, where u is the unshifted and s is the Doppler-shifted γ-ray peak area, is plotted against the target-stopper distance. The data points have been corrected for detector efficiency and solid angle effects. The decay curve includes allowance for cascade feeding as well as deorientation effects.

Fig. 7. Decay curves for the 8^+ and 6^+ levels in ^{170}Er for 120 MeV and 140 MeV bombarding energies.

Fig. 8. Decay curves for the 8^+ and 6^+ levels in ^{174}Yb for 125 MeV and 140 MeV bombarding energies.

Fig. 9. Decay curves for the 4^+ levels in ^{170}Er and ^{174}Yb for bombarding energies shown.

Fig.10. Summary of $B(E2)/B(E2)_{rot}$ from the present experiment and other results from DBLS measurements: a) ref.[33], b) ref.[13] and c) ref.[14]. The $B(E2;0\rightarrow2)$ is assumed to be rotational and is tabulated in table 2.

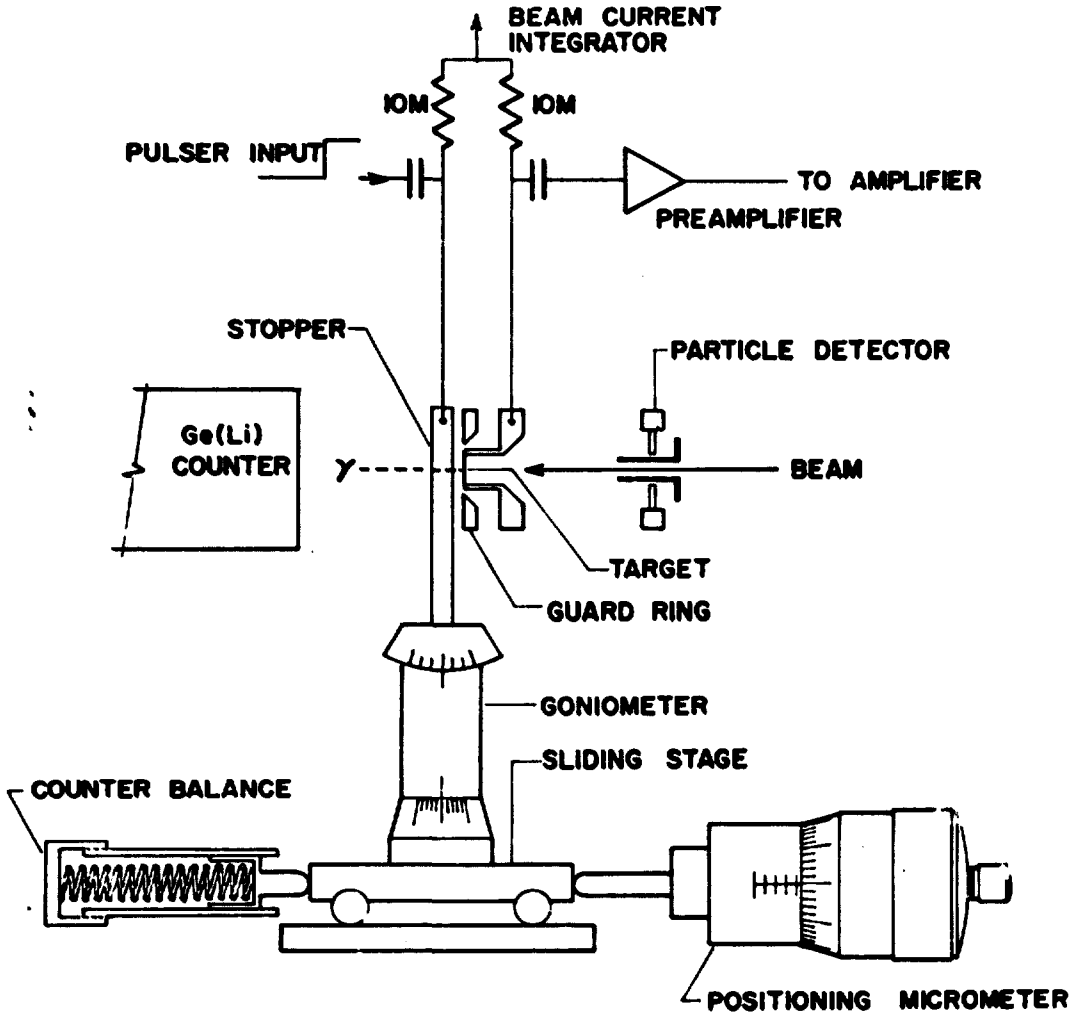
BEAM CURRENT
INTEGRATOR
IOM
IOM
PULSER INPUT
TO AMPLIFIER
PREAMPLIFIER
STOPPER
PARTICLE DETECTOR
Ge(Li)
COUNTER
γ
BEAM
TARGET
GUARD RING
GONIOMETER
SLIDING STAGE
COUNTER BALANCE
POSITIONING MICROMETER

Fig. 1

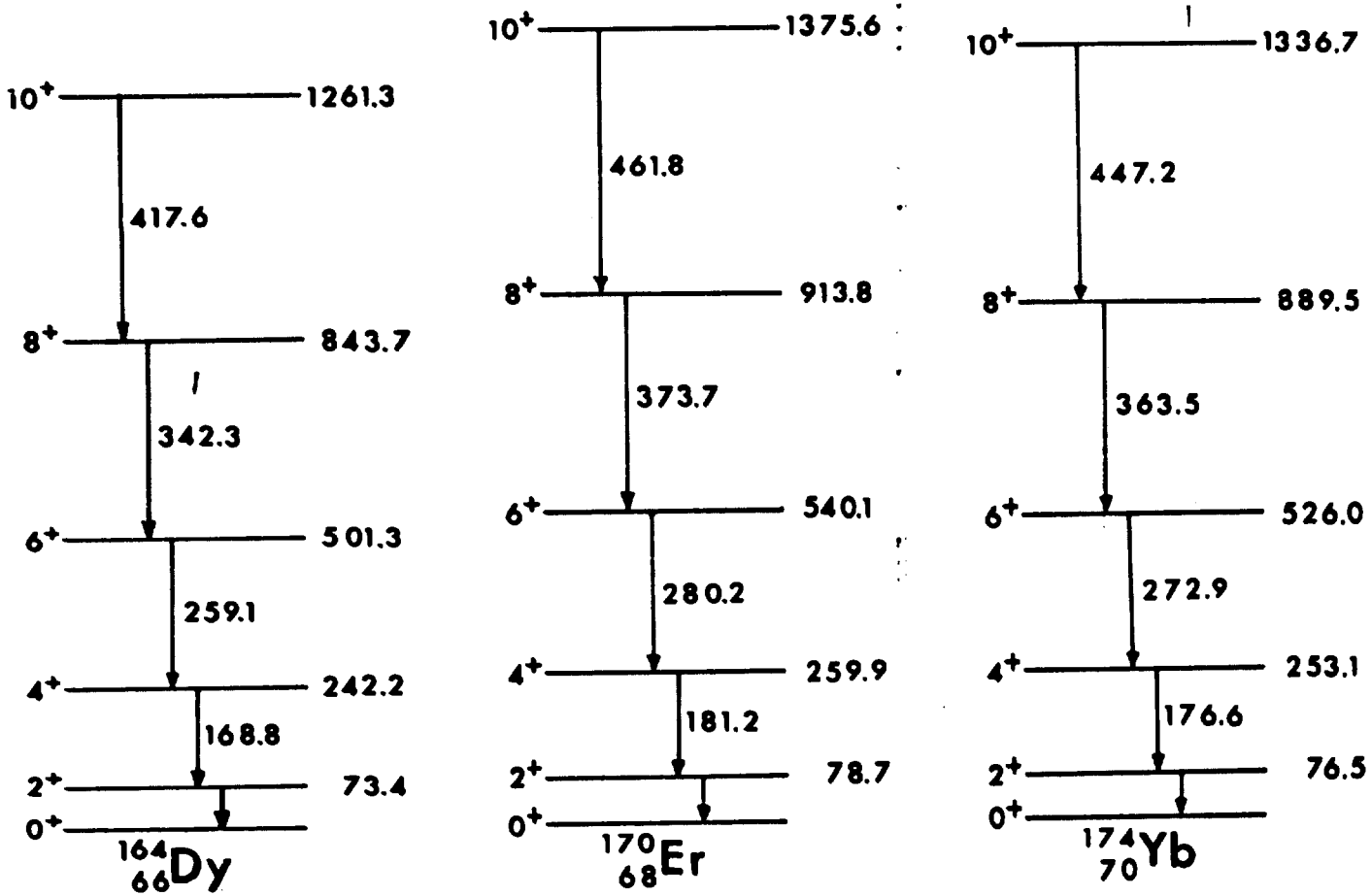
10+
1261.3
417.6
8+
843.7
342.3
6+
501.3
259.1
4+
242.2
168.8
2+
73.4
0+
164 66 Dy
10+
1375.6
461.8
8+
913.8
373.7
6+
540.1
280.2
4+
259.9
181.2
2+
78.7
0+
170 68 Er
10+
1336.7
447.2
8+
889.5
363.5
6+
526.0
272.9
4+
253.1
176.6
2+
76.5
0+
174 70 Yb

Fig. 2

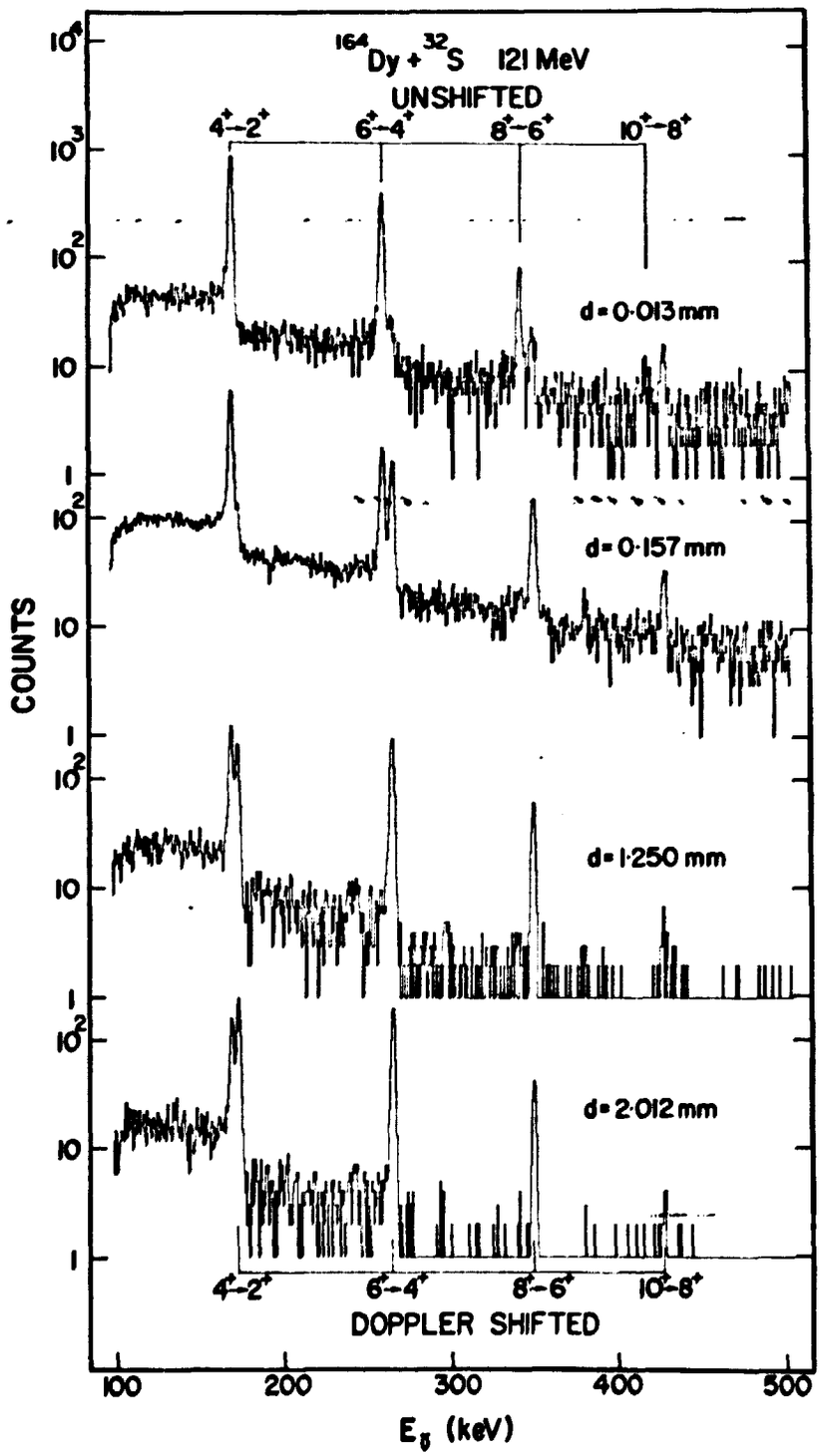
$^{164}Dy + ^{32}S$ 121 MeV
UNSHIFTED
4^+-2^+
6^+-4^+
8^+-6^+
10^+-8^+
d = 0·013 mm
d = 0·157 mm
d = 1·250 mm
d = 2·012 mm
COUNTS
4^+-2^+
6^+-4^+
8^+-6^+
10^+-8^+
DOPPLER SHIFTED
100
200
300
400
500
E_γ (keV)

Fig. 3

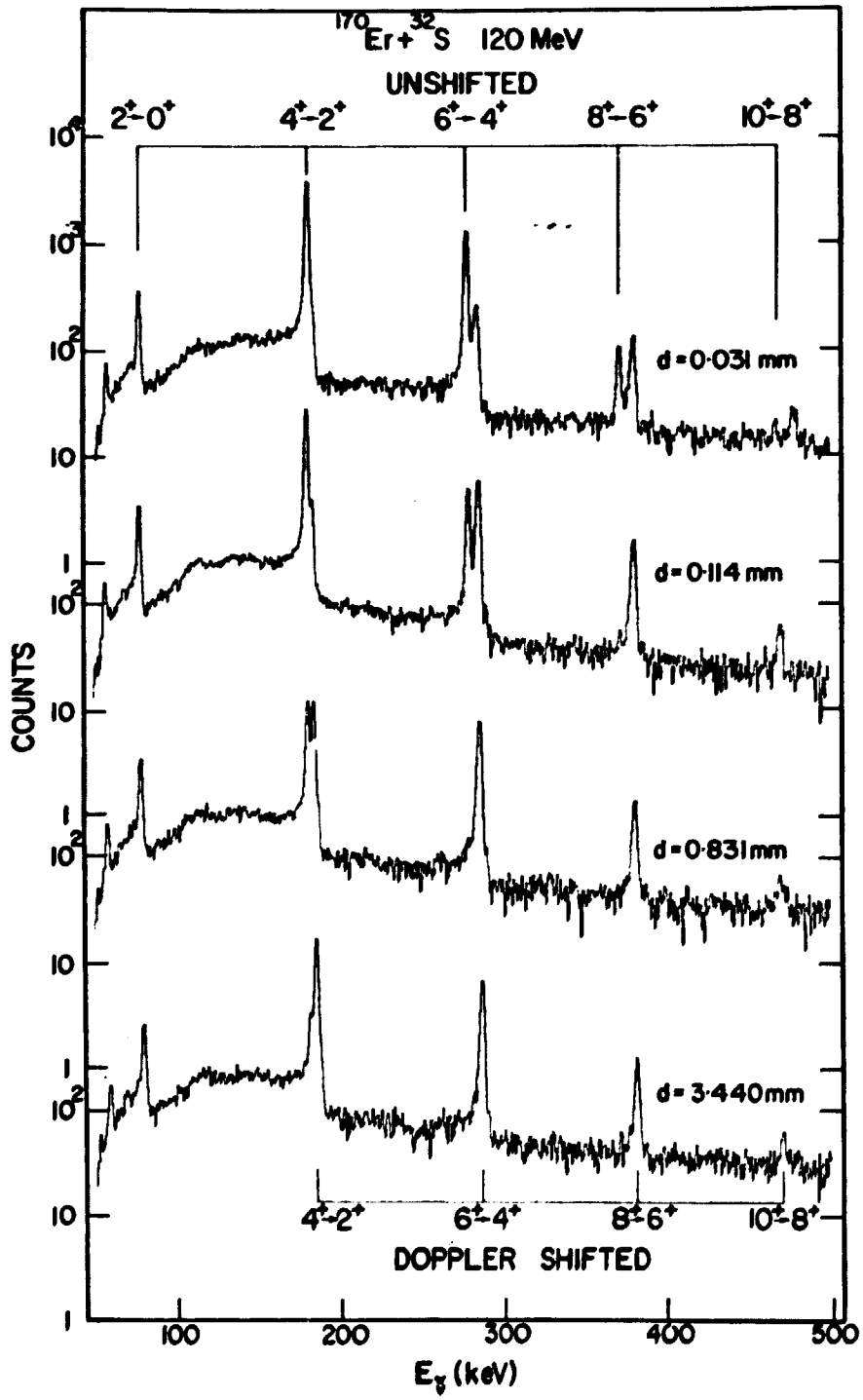
$^{170}Er + ^{32}S$ 120 MeV
UNSHIFTED
2^+-0^+
4^+-2^+
6^+-4^+
8^+-6^+
10^+-8^+
d = 0·031 mm
d = 0·114 mm
d = 0·831 mm
d = 3·440 mm
4^+-2^+
6^+-4^+
8^+-6^+
10^+-8^+
DOPPLER SHIFTED
COUNTS
E_γ (keV)
100
200
300
400
500

Fig. 4

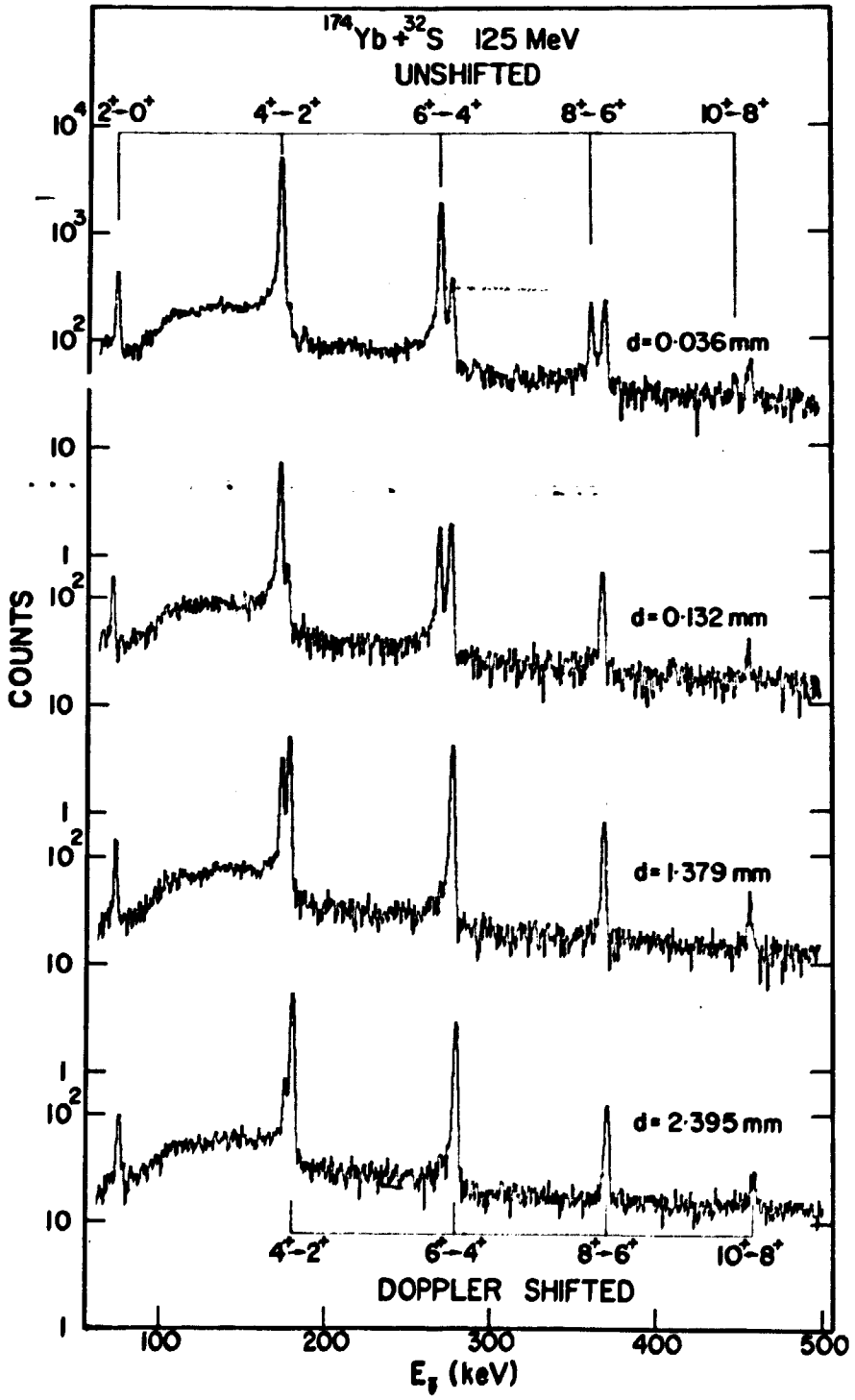
$^{174}Yb + ^{32}S$ 125 MeV
UNSHIFTED
2^+-0^+
4^+-2^+
6^+-4^+
8^+-6^+
10^+-8^+
d=0·036mm
d=0·132mm
d=1·379mm
d=2·395mm
COUNTS
4^+-2^+
6^+-4^+
8^+-6^+
10^+-8^+
DOPPLER SHIFTED
E_γ (keV)

Fig. 5

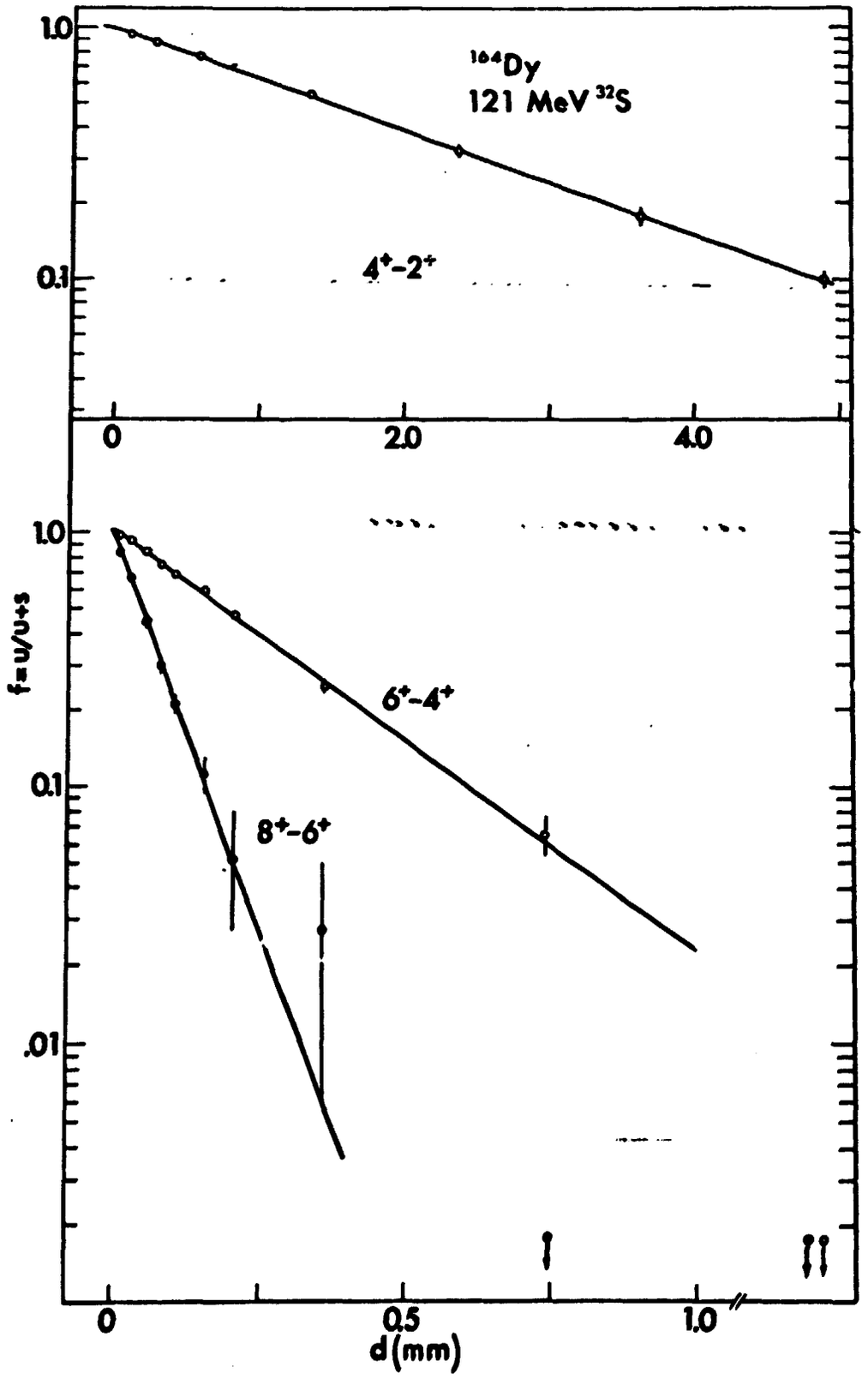

Fig. 6

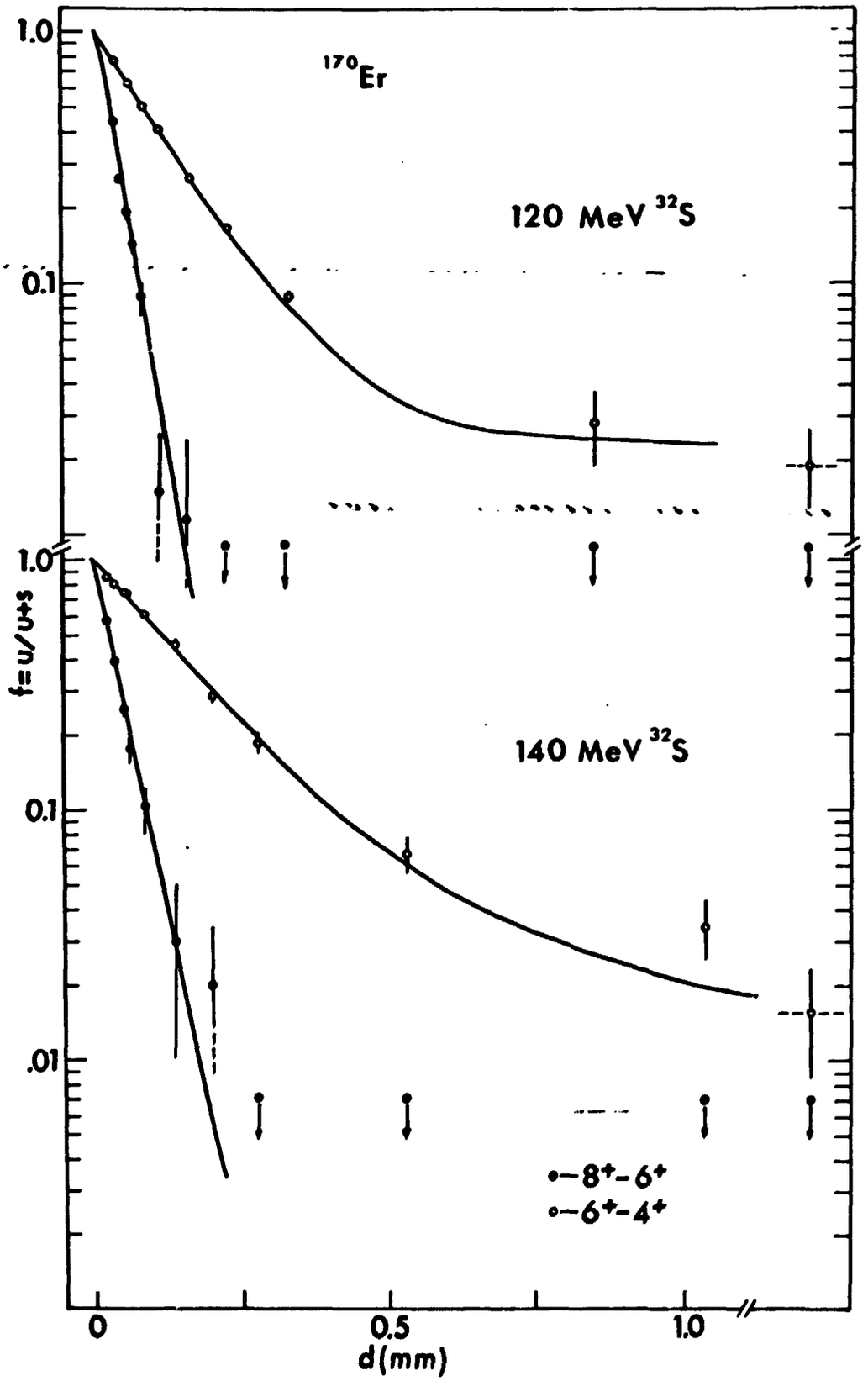

fig. 7

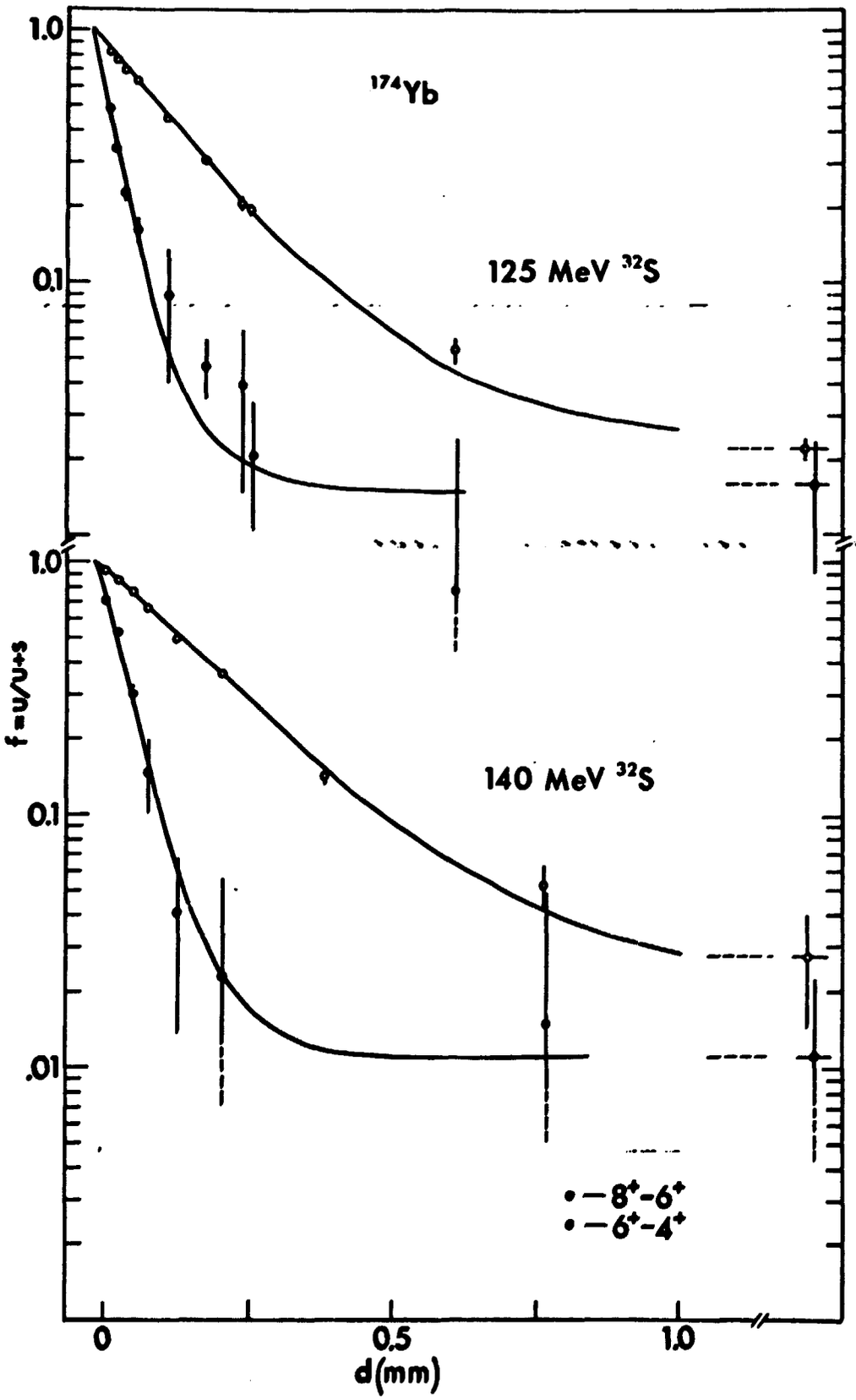

Fig. 8

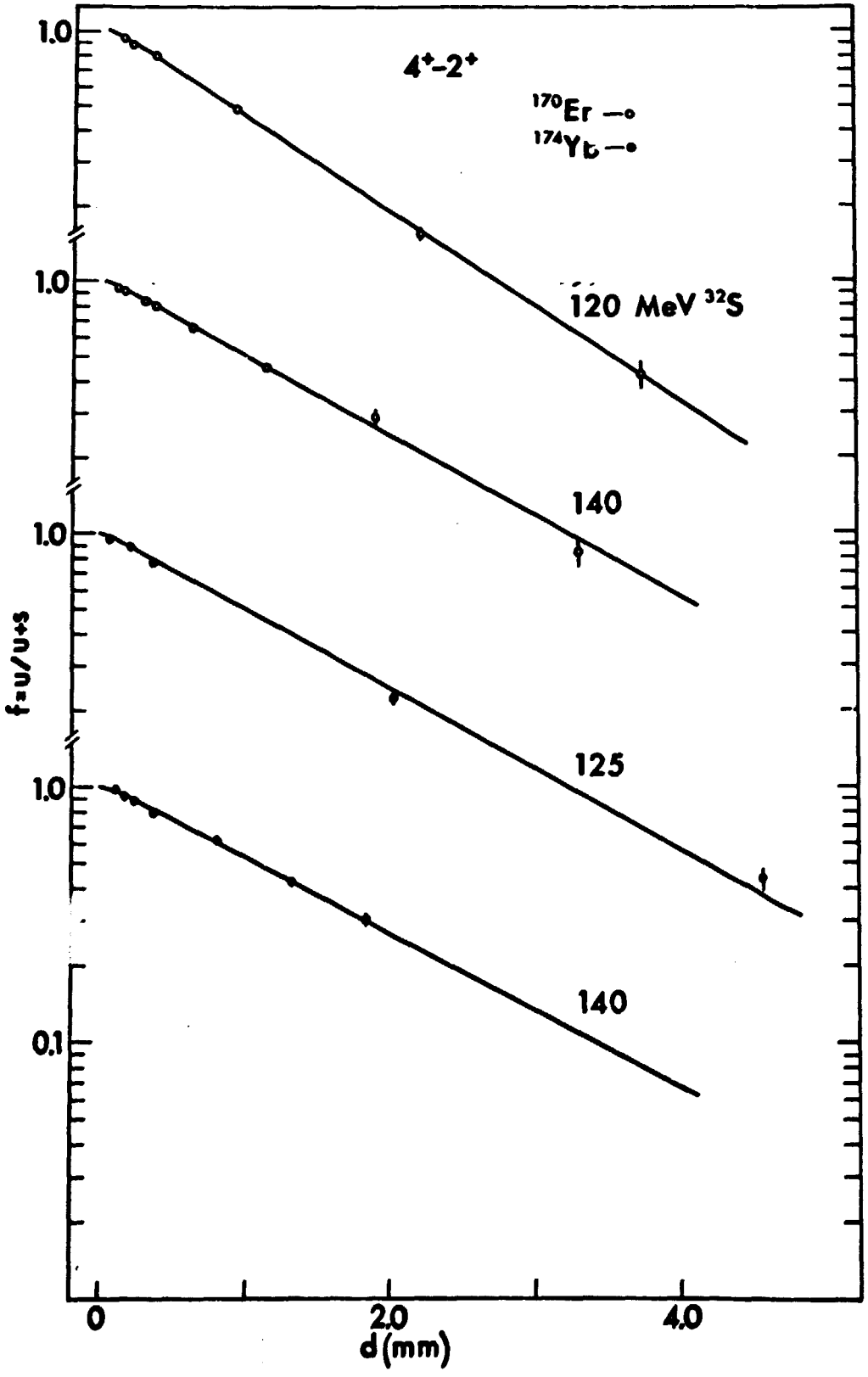
4⁺-2⁺
170Er —o
174Yb —•
120 MeV 32S
140
125
140
1.0
1.0
1.0
1.0
0.1
f=U/U+S
0
2.0
4.0
d(mm)

Fig. 9

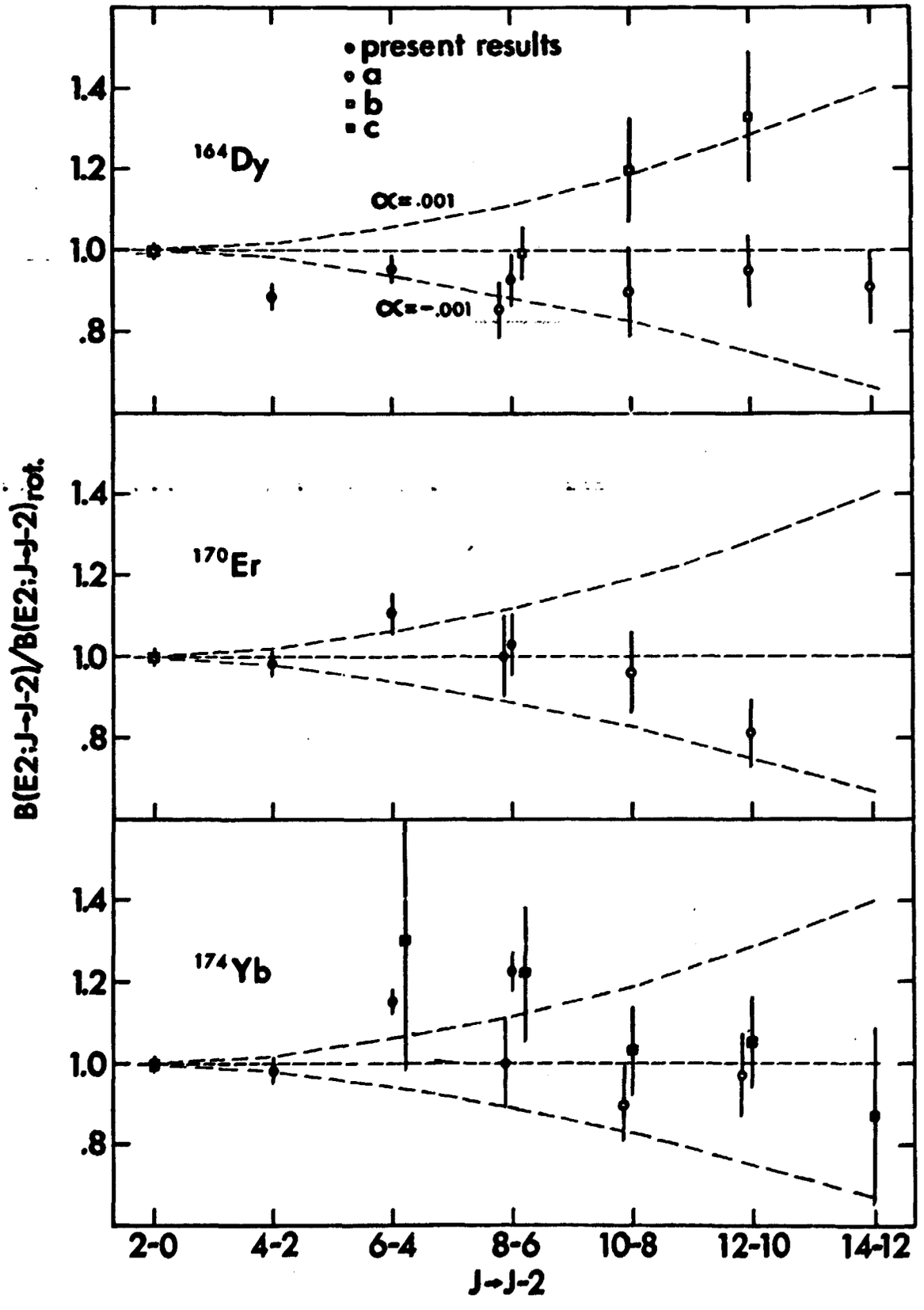
• present results
• a
▪ b
▪ c
^{164}Dy
α=.001
α=-.001
^{170}Er
^{174}Yb
1.4
1.2
1.0
.8
B(E2:J→J-2)/B(E2:J→J-2)$_{rot.}$
2-0
4-2
6-4
8-6
10-8
12-10
14-12
J→J-2

Fig. 10